Materials Science and Engineering C 33 (2013) 4313–4322

Contents lists available at ScienceDirect

Materials Science and Engineering C

journal homepage: www.elsevier.com/locate/msec

Development of bimetal-grown multi-scale carbon micro-nanofibers as an immobilizing matrix for enzymes in biosensor applications

Amit R. Hood [a], Neelam Saurakhiya [b], Dinesh Deva [b], Ashutosh Sharma [a,b], Nishith Verma [a,c,*]

[a] Department of Chemical Engineering, Indian Institute of Technology, Kanpur, India
[b] DST Unit on Nanosciences, Kanpur, 208016, India
[c] Center for Environmental Science and Engineering, Kanpur 208016, India

ARTICLE INFO

Article history:
Received 30 December 2012
Received in revised form 28 April 2013
Accepted 19 June 2013
Available online 28 June 2013

Keywords:
Activated carbon microfibers
Carbon nanofibers
Glucose oxidase
Immobilization
Biosensor

ABSTRACT

This study describes the development of a novel bimetal (Fe and Cu)-grown hierarchical web of carbon micro-nanofiber-based electrode for biosensor applications, in particular to detect glucose in liquids. Carbon nanofibers (CNFs) are grown on activated carbon microfibers (ACFs) by chemical vapor deposition (CVD) using Cu and Fe as the metal catalysts. The transition metal-fiber composite is used as the working electrode of a biosensor applied to detect glucose in liquids. In such a bi-nanometal-grown multi-scale web of ACF/CNF, Cu nanoparticles adhere to the ACF-surface, whereas Fe nanoparticles used to catalyze the growth of nanofibers attach to the CNF tips. By ultrasonication, Fe nanoparticles are dislodged from the tips of the CNFs. Glucose oxidase (GOx) is subsequently immobilized on the tips by adsorption. The dispersion of Cu nanoparticles at the substrate surface results in increased conductivity, facilitating electron transfer from the glucose solution to the ACF surface during the enzymatic reaction with glucose. The prepared Cu-ACF/CNF/GOx electrode is characterized for various surface and physicochemical properties by different analytical techniques, including scanning electron microscopy (SEM), electron dispersive X-ray analysis (EDX), Fourier-transform infrared spectroscopy (FTIR), BET surface area analysis, and transmission electron microscopy (TEM). The electrochemical tests show that the prepared electrode has fast response current, electrochemical stability, and high electron transfer rate, corroborated by CV and calibration curves. The prepared transition metal-based carbon electrode in this study is cost-effective, simple to develop, and has a stable immobilization matrix for enzymes.

1. Introduction

For more than two decades, amperometric biosensors using enzymes are an active area of research for the detection of glucose in human serum [1,2]. In such biosensors, the enzyme is directly immobilized onto the electrode. As a result, the amperometric output signal is amplified because of direct electron transfer between the redox center of the enzyme and the electrode. In this context, physically or chemically modified carbon nanotube (CNT)- and carbon nanofiber (CNF)-based electrodes have shown substantial improvements in their amperometric performance. A review of such CNT- and CNF-based biosensors can be found in the literature [3,4]. Some examples are the Pt nanoparticle-supported CNTs [5,6], CNTs dispersed in glassy carbon [7], and Pt nanoparticle–graphene nanocomposite [8]. However, these electrodes are complicated to fabricate and are relatively expensive because of the noble metals, including gold and platinum, used in the fabrication. Herein, it may be mentioned that there are electrodes based on non-carbon materials also, including polymers and silica, prepared for glucose biosensors [9–11]. However, such electrodes are coated with expensive gold or platinum noble metals as well.

Activated carbon microfibers (ACFs) have been used as adsorbents and support for metal catalyst nanoparticles in several environmental remediation applications [12–16]. Recently, ACF has been used as a substrate to grow carbon nanofibers (CNFs) by catalytic chemical vapor deposition (CCVD) using a suitable transition metal (Ni/Fe/Cu). The multi-scale web of carbon micro and nanofibers (ACF/CNF) has been found to be a more efficient adsorbent than ACFs alone [17–21]. The ACF/CNF composite is also a good thermal and electrical conductor. Therefore, this material, which is the focus of the present study, can potentially be used as the working electrode of glucose biosensors.

In this study, the ACF/CNF composite is prepared using a bimetal of Cu and Fe instead of either metal alone. Fe nanoparticles catalyze the growth of CNFs by the tip-growth mechanism, whereas Cu nanoparticles remain dispersed in the ACF substrate. The hierarchical

* Corresponding author at: N. Verma, Department of Chemical Engineering, Indian Institute of Technology, Kanpur, India. Tel.: +91 512 2596124; fax: +91 512 2590104.
E-mail address: nishith@iitk.ac.in (N. Verma).

0928-4931/$ – see front matter © 2013 Elsevier B.V. All rights reserved.
http://dx.doi.org/10.1016/j.msec.2013.06.030

web of ACF/CNF is ultrasonicated to open the CNF tips by dislodging the Fe nanoparticles. Glucose oxidase (GOx) is immobilized on the tips by adsorption. With Cu nanoparticles dispersed in the substrate, the prepared composite material is shown to exhibit significantly high electron transfer rate during the enzymatic reaction with glucose in liquid and thus is a potential candidate for the working electrode of glucose biosensors. Thus, the bimetals have different roles in the detection of glucose. Fe-nanoparticles act as the CVD catalyst for growing CNFs. The grown nanofibers are used to immobilize GOx by adsorption. The CNFs also act as the electrode to directly transfer electrons during the enzymatic reaction with glucose. Cu-nanoparticles dispersed on the substrate ACF enhance the conductivity of the substrate, facilitating electron transfer from the glucose solution to the ACF surface.

2. Materials and method

The phenolic resin precursor based micron size-ACF was procured from Nippon Kynol Inc., Japan. The chemicals used for the impregnation of ACFs, $Cu(NO_3)_2 \cdot 3H_2O$ (purity >99%), Fe $(NO_3)_3.9H_2O$ (purity > 99.9%), Ni $(NO_3)_2 \cdot 6H_2O$, and the surfactant reagent, sodium dodecyl sulfate (SDS) (Purity > 99%) were purchased from Merck, Germany. Different gases, hydrogen (purity > 99.999%), nitrogen (purity > 99.999%), and acetylene (C_2H_2) (purity > 99.999%) were purchased from BOC Gases, India. GOx derived from *Aspergillus niger* (activity > 300 U/mg) were purchased from Calbiochem, Germany. The high purity grades Bradford reagent and β-D-Glucose (>80%) were purchased from Sigma-Aldrich, Germany and TCI, Tokyo, respectively. O-dianisidine (>99%) and peroxidase (>250 U/mg) were purchased from Alfa Aesar, UK. The remaining reagents required for preparing buffer solutions, KH_2PO_4, K_2HPO_4, NaCl crystals, glacial acetic acid and sodium acetate, were purchased from Merck, India. All chemicals were prepared in de-ionized (DI) water.

2.1. Synthesis of bimetal ACF/CNF

Fig. 1 describes the steps involved in the preparation of the ACF/CNF-based working electrode for glucose biosensors. Fe-metal nanoparticles (shown in red) that are used to catalyze the CNF growth on the ACF substrate are on the CNF tips, whereas Cu-metal nanoparticles (shown in black) are dispersed in the ACFs (Fig. 1a). The hierarchical web of ACF/CNF is ultrasonicated to open the CNF tips by dislodging the Fe nanoparticles (Fig. 1b). Next, glucose oxidase (GOx) (shown in yellow) is immobilized on the tips (Fig. 1c). The Cu nanoparticles, which remain adhered to the ACF-substrate, render the composite material more electrically conductive. As a result, the electron transfer rate of the composite material used as the counter electrode of the biosensor is higher during the enzymatic reaction with glucose in solution (Fig. 1d), as shown later in this manuscript.

2.1.1. Pretreatment of ACFs

The as-received samples of ACF were leached for 2 h in 0.03 M nitric acid at 80 °C to remove any undesirable ions, such as chloride, nitrate, and phosphate ions. After leaching, the ACFs were washed several times with DI water until the surface of the ACFs became neutral (pH ~7). Next, the ACFs were dried for 6 h in static air at room temperature (30 ± 5 °C), then for 12 h in an oven at 120 °C and for another 12 h in vacuum at 200 °C to remove any entrapped gases from the pores of ACFs.

2.1.2. Impregnation of ACF with metal nitrates

The impregnation of ACFs was conducted by the wet incipient method. The salts of Fe and Cu nitrates, used as the precursors of Fe and Cu metals in ACF, respectively, were dispersed in DI water. Based on previous results [20], the concentration of metallic salts in the solution was adjusted to 0.4 M for impregnating ACFs. At concentrations in excess of 0.4 M, the pores of ACFs were found to be plugged with the salts. SDS (0.3% w/w) was added to the impregnating solution to produce mono-dispersed nanoparticles of the metallic salts and to increase the transfer of the salts without agglomeration to the ACF surface.

The set-up for impregnation consisted of a glass tube (I.D. = 20 mm, L = 90 mm) mounted inside a cylindrical glass shell (I.D. = 35 mm, L = 13 cm). The inner tube was perforated. ACF was wrapped on it. One end of the tube was sealed. The impregnating salt solution was continuously delivered into the tube via a peristaltic pump (speed = 110 rpm). The solution flowed into the tube and then radially outward into the shell through the wrapped ACF. The impregnation was conducted for 6 h. Some samples of ACFs impregnated with Fe and Ni or Ni and Cu, were also prepared for comparison purposes. As shown

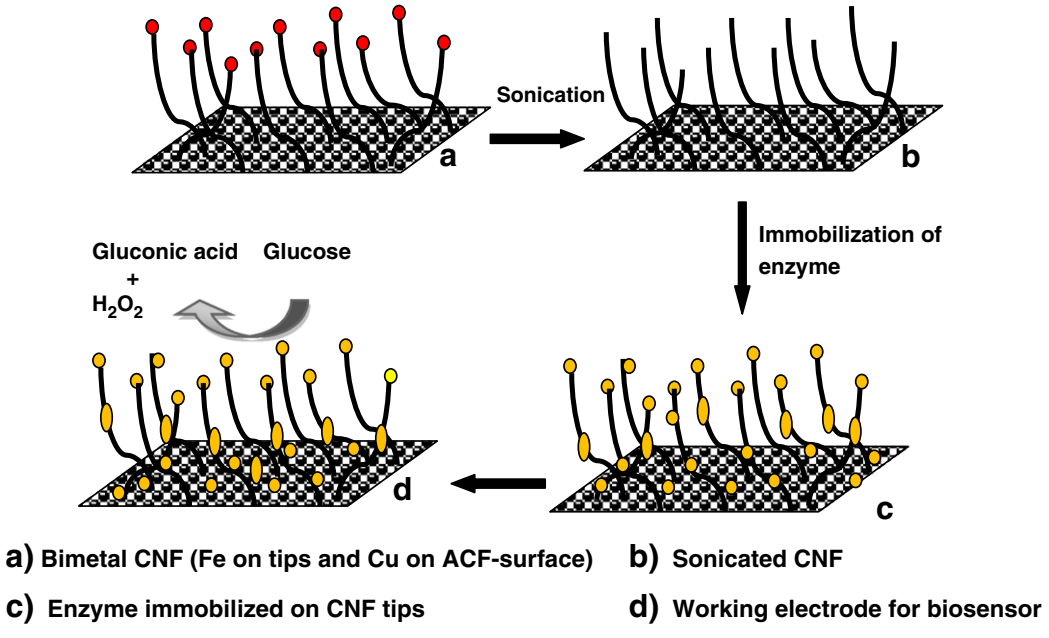

Fig. 1. Schematic of the proposed bimetal CNF-based electrode for glucose biosensor.

later in this manuscript, the combination of Fe and Cu was preferred for uniform and dense growth of ACFs, with Cu adhered to the ACF surface and Fe attached to the CNF tips. Samples were also prepared by impregnating ACFs with Fe and Cu salts of different molar ratios (1:3, 1:1, and 3:1) to determine the optimum ratio of the metals in the ACF/CNF composites for the maximum yield of CNFs.

2.1.3. Calcinations, reduction, and CVD of metal-impregnated ACFs

The ACFs impregnated with metal salts were first dried for 6 h in static air at room temperature and then for 12 h in the oven at 100 °C to vaporize the volatile solvent from the ACFs. The details of the experimental set-up used for calcinations, reduction, and CVD are reported in the literature [20]. Briefly, a short U-shaped tube was fitted to the bottom end of a vertical stainless steel (SS) tube (ID = 25 mm) fitted coaxially in a vertical quartz shell (ID = 150 mm). A perforated tube (ID = 30 mm), closed at one end, was fitted to the bottom end of the U-tube. The bimetal-impregnated ACF samples were wrapped over the perforated tube. Different process gases (N_2 for calcination, H_2 for reduction, and N_2 laden with benzene for CVD) flowed downward through the vertical SS tube, upward through the U-tube and then through the wrapped ACFs into the quartz shell.

Fe and Cu nitrate salts dispersed in ACFs were converted into their respective oxides by calcinations for 4 h at 400 °C in N_2 atmosphere. Next, the oxides of the bimetals were converted into their respective metallic state by the reduction of the calcined samples at 550 °C for 2 h in a H_2 atmosphere (flow rate = 0.2 standard liters per min [slpm]). The Fe and Cu dispersed ACFs thus prepared were used as the substrate to grow CNFs by CVD. The liquid benzene was used as the source of carbon. A Freon refrigeration unit (R-15) was used to set the temperature (8 °C) of the liquid. N_2 was bubbled through the liquid to the CVD reactor. The CVD temperature was set at 800 °C. At this temperature, Fe catalyzed the growth of CNFs by the decomposition of benzene vapor, but Cu did not. After CVD, the system was allowed to cool using N_2 gas. Different CVD temperatures were required to grow CNFs for the other combinations of bimetals (Fe and Ni or Ni and Cu).

2.2. Fabrication of sensor-electrode and electrochemical cell

Ultrasonication was performed on the prepared multi-scale web of carbon micro-nanofibers in the acidic medium (0.05 M HNO_3) for 5 min to dislodge the Fe nanoparticles attached to the CNF tips. The ACF/CNF composite containing Cu nanoparticles dispersed in ACFs and CNFs with open pore-mouth was used as the immobilization matrix for the enzyme. Immobilization was conducted by dispersing the sonicated samples in the acetate solution containing GOx (concentration = 1 mg/ml). The acetate solution was used as a buffer (pH = 4.5). The adsorption of GOx on the composite material was carried out for 24 h in a shaker at 5 °C. As the working pH was close to the isoelectric point of GOx, it yielded a good loading (40 mg/g) of GOx on the CNFs. The concentration of GOx was determined by the Bradford assay method using UV–Vis spectroscopy. After adsorption, the sample was washed with phosphate buffer (PBS) solution (pH = 7.2) to remove the un-immobilized enzyme, and then, it was dried for 6 h in static air at room temperature. Next, the enzyme-immobilized Cu-ACF/CNF composite was tested as a working electrode in the 3-electrode assembly of an electrochemical cell in which Ag/AgCl in saturated KCl salt bridge electrode was used as the reference electrode and Pt as the counter electrode.

Table 1a
AAS analysis of metals loading on ACFs after impregnation.

Sample (1:1)	Fe-loading (g/g)	Cu-loading (g/g)	Ni-loading (g/g)
Ni–Cu	–	0.092	0.367
Ni–Fe	0.060	–	0.348
Fe–Cu	0.212	0.150	–

Table 1b
AAS analysis of Fe–Cu loading on ACFs after impregnation.

Sample	Fe loading (g/g)	Cu loading (g/g)
Fe–Cu (1:3)	0.074	0.391
Fe–Cu (1:1)	0.212	0.150
Fe–Cu (3:1)	0.390	0.148

The prepared Cu-ACF/CNF/GOx composite was supported on a circular Teflon solid frame (exposed area = 78.5 mm^2). This assembly was used as the counter electrode of the electrochemical biosensor. PBS solution (pH = 7.2) was used as an electrolyte medium. The amperometric (I–t) measurements at constant applied potential and cyclic voltammetry (CV) characteristics (potential range = −2 V–2 V) were conducted using an Autolab PGSTAT (Model 302) potentiostat/galvanostat. To obtain the amperometric measurements, 0.7 V potential was applied between the working electrode and the reference electrode. The calibration curve for the glucose sensor was obtained by measuring the steady-state response current corresponding to different glucose concentrations over the range from 0.5 mM to10 mM. Samples of plain ACF and ACF-Fe/CNF (web of ACF/CNF prepared by using single metal, Fe only) were also tested for comparison purposes.

3. Surface characterization

The prepared samples were analyzed using several techniques, including atomic absorption spectroscopy (AAS), Fourier transform infrared spectroscopy (FTIR), and scanning electron microscopy (SEM). The AAS (Varian AA-240, USA) analysis of the impregnating solution was carried out to determine the metal loadings on ACF. The adsorption/desorption isotherms and pore volumes of the materials were determined using nitrogen at 77 K by the Autosorb-1C (Quantachrome, USA) instrument. The total surface area and pore volume were determined using the Brunauer–Emmet–Teller (BET) equation and the 22-point method, respectively. The pore size distribution (PSD) was obtained by the Barret–Joyner–Halenda (BJH) method. The surface functional groups of the prepared carbon composites were determined by FTIR (Tensor 27, Bruker, Germany) over the wave-numbers ranging from 400 to 4000 cm^{-1}, using the attenuated total reflectance (ATR) accessory with the germanium (Ge) crystal. The surface morphology of CNFs before and after adsorption of enzyme was examined using field emission SEM (Supra 40 VP, Zeiss, Germany). The metals dispersed in ACF/CNF were determined by electron dispersive X-ray spectroscopy (EDX) (INCA Energy system, UK). The transmission electron microscopy (TEM) (FEITecnai 20 U) analysis of the prepared bimetals-grown CNF samples was conducted before and after adsorption of GOx to confirm its immobilization on the CNFs. The resistivity of the prepared material for the

Table 2
BET surface area and PSD of the prepared samples.

SAMPLE	S_{BET} (m^2/g)	Pore volumes (cc/g)			
		V_{total}	Micro	Meso	Macro
ACF	1497	0.809	0.701	0.057	0.044
Fe–Cu (3:1) ACF (post-impregnation)	817	0.412	0.345	0.048	0.020
Fe–Cu ACF (post-calcination)	1099	0.584	0.509	0.051	0.025
Fe–Cu ACF (post-reduction)	1261	0.669	0.583	0.039	0.046
Fe–Cu ACF/CNF	252	0.328	0.171	0.129	0.030

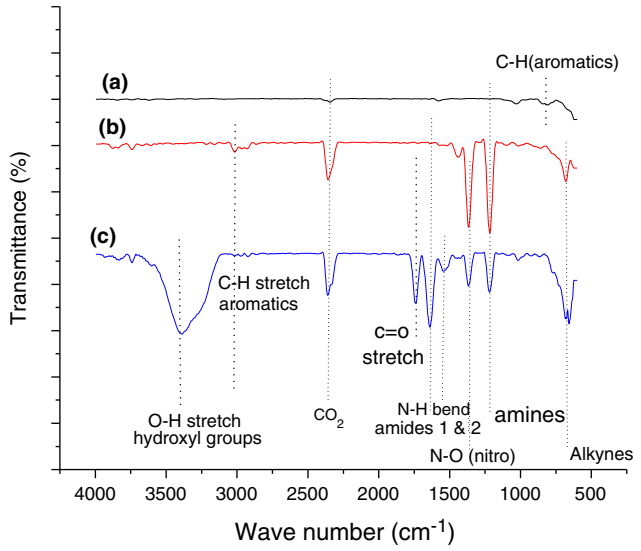

Fig. 2. FT-IR spectra of (a) ACF, (b) Cu-ACF/CNF, and (c) Cu-ACF/CNF adsorbed with enzyme.

electrode was measured by the I–V source-meter (Keithley 6221, USA).

4. Results and discussion

4.1. Metals-loading on ACF surface

The samples of impregnating solutions containing salts of different combinations of metals, i.e., Ni and Fe, Fe and Cu, or Cu and Ni were collected for the AAS analysis in small glass bottles before and after impregnation of ACFs. A fixed volume (10 μL) of the solutions was pipetted into a 100 ml volumetric flask, and the volume was adjusted to 100 ml using DI water.

Table 1a shows the AAS data for different combinations of bimetal used in the identical molar ratio (1:1). The ACFs impregnated with the combination of Fe- and Cu-salts contained significant loading for both metals compared to those of the other combinations (Ni and Cu or Fe and Ni). In general, fine dispersions and comparable loadings of both metals on ACF were required to grow dense CNFs that had high electrical conductivity. As discussed later in this manuscript, the web prepared using Fe and Cu contained a uniform and dense growth of CNFs, with Fe attached to CNF tips, and Cu dispersed in the substrate ACF.

As previously mentioned, samples of Fe–Cu ACFs were prepared also by using different molar ratios (1:1, 1:3 and 3:1) of Fe and Cu in the impregnating solutions. Table 1b summarizes the corresponding AAS data. As discussed later in this manuscript, the ACF prepared with Fe and Cu in the molar ratio of 3 to 1 yielded ACF/CNF composites that had a dense growth of fibers and a high conductivity; therefore, it was used as the electrode material in this study.

4.1.1. BET surface area and PSD

The BET surface area and pore volume of the samples were calculated from the N_2adsorption/desorption isotherms. All samples were degassed for 8 h at 200 °C under vacuum before the measurement. Table 2 summarizes the data for the samples at the various stages of preparation. The substrate ACF had significantly large BET surface area (~1500 m^2/g). After impregnation with the metal-salts, the surface area decreased. Calcinations and reduction, however, resulted in increased surface area because the pores opened up as the metal salts were converted into oxide and then into the metallic state. CNFs had less BET area than expected because of N_2 used as the probe molecules for the BET measurement. N_2 molecules were unable to penetrate the

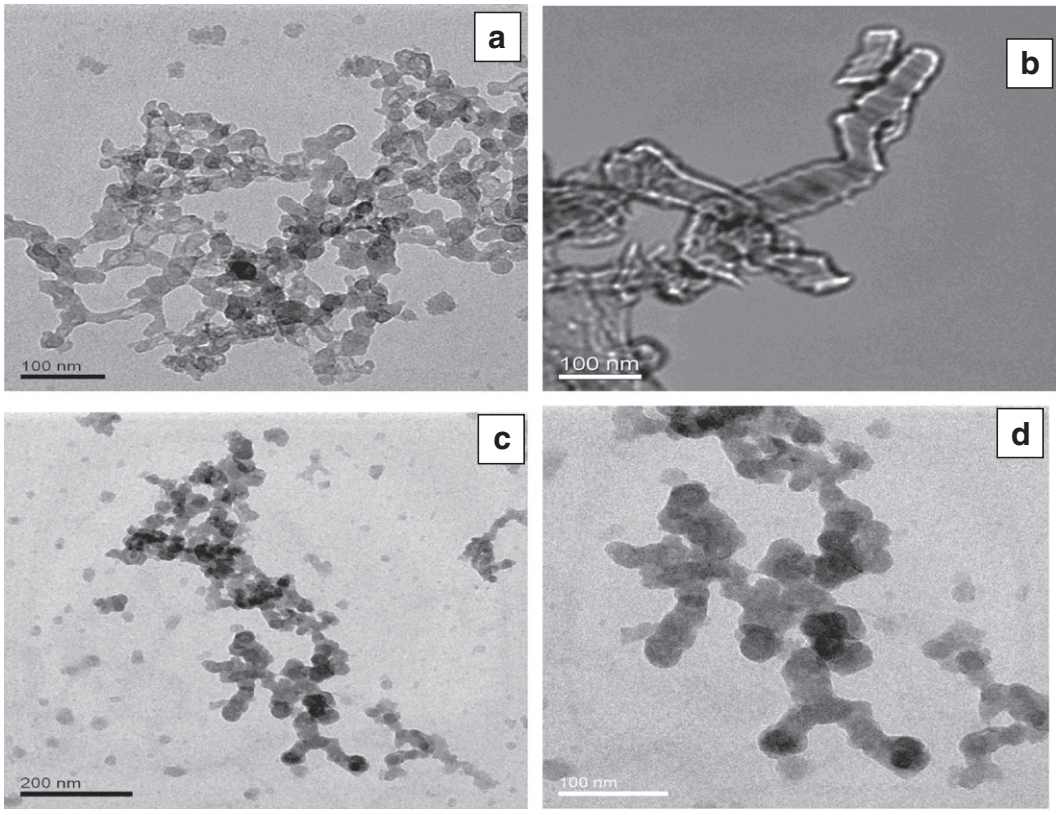

Fig. 3. TEM images of Cu-ACF/CNF: before (a, b) and after (c, d) enzyme immobilization.

micropores of the grown nanofibers [22]. Considering that GOx is a dimeric globular protein having the overall dimensions of approximately 6.0 nm × 5.2 nm × 6.7 nm, micro-mesoporous materials are considered to be a suitable immobilizing matrix for the adsorption of GOx [23]. As observed from Table 2, the CNFs contain an adequate level of the required micro-mesopores for the adsorption of enzyme.

4.1.2. FTIR analysis

Prior to the measurements, the background spectrum was recorded. Next, the resolution was set to 4 cm^{-1}. A total of 100 scans were collected for each sample. Fig. 2 describes the FTIR spectra of the ACF, Cu-ACF/CNF, and Cu-ACF/CNF immobilized with enzyme. The peaks at 2350 cm^{-1}, 1225 cm^{-1}, and 830 cm^{-1} were observed in the ACF spectra, corresponding to the surface entrapped CO_2, N–H stretch of amines, and C–H "oop" stretch of aromatics, respectively. These functional groups are inherently present in the ACFs. In the Cu-ACF/CNF samples, peaks at 3020 cm^{-1} corresponded to the C–H stretch of aromatics, 1350 cm^{-1} corresponded to the N–O symmetric stretch of nitro compound, 1225 cm^{-1}correspondedtothe N–H stretch of amines, and 660 cm^{-1}correspondedtothe C≡C bend of alkynes. The peak observed at 2350 cm^{-1} is attributed to the atmospheric CO_2 molecules present in the chamber. The peak corresponding to the C–H stretching is attributed to the formation of graphene layers of CNF produced after CVD, whereas the N–O symmetric stretching of the nitro compound is attributed to the sonication of CNFs in HNO_3 medium.

In the enzyme-adsorbed samples of Cu-ACF/CNF, the peak observed at 3390 cm^{-1} is attributed to the O–H stretching of hydroxyl groups of the GOx molecule. The peaks observed at 1650 cm^{-1} and 1550 $cm^{-1}$are assigned to the N–H bends of amide and amide II of GOx molecule, respectively. The spectra confirmed the adsorption of enzyme on the surface of CNFs. The peak was also observed at 1750 cm^{-1}, attributed to the C═O stretch of carboxyl group because of the acetate buffer used for preparing the enzyme solution [24].

4.1.3. TEM analysis of GOx immobilized Cu-ACF/CNF

The morphology of the sonicated samples before and after the immobilization of enzyme was characterized by TEM. Fig. 3(a)and (b) show the images of CNFs before the adsorption of enzyme. The

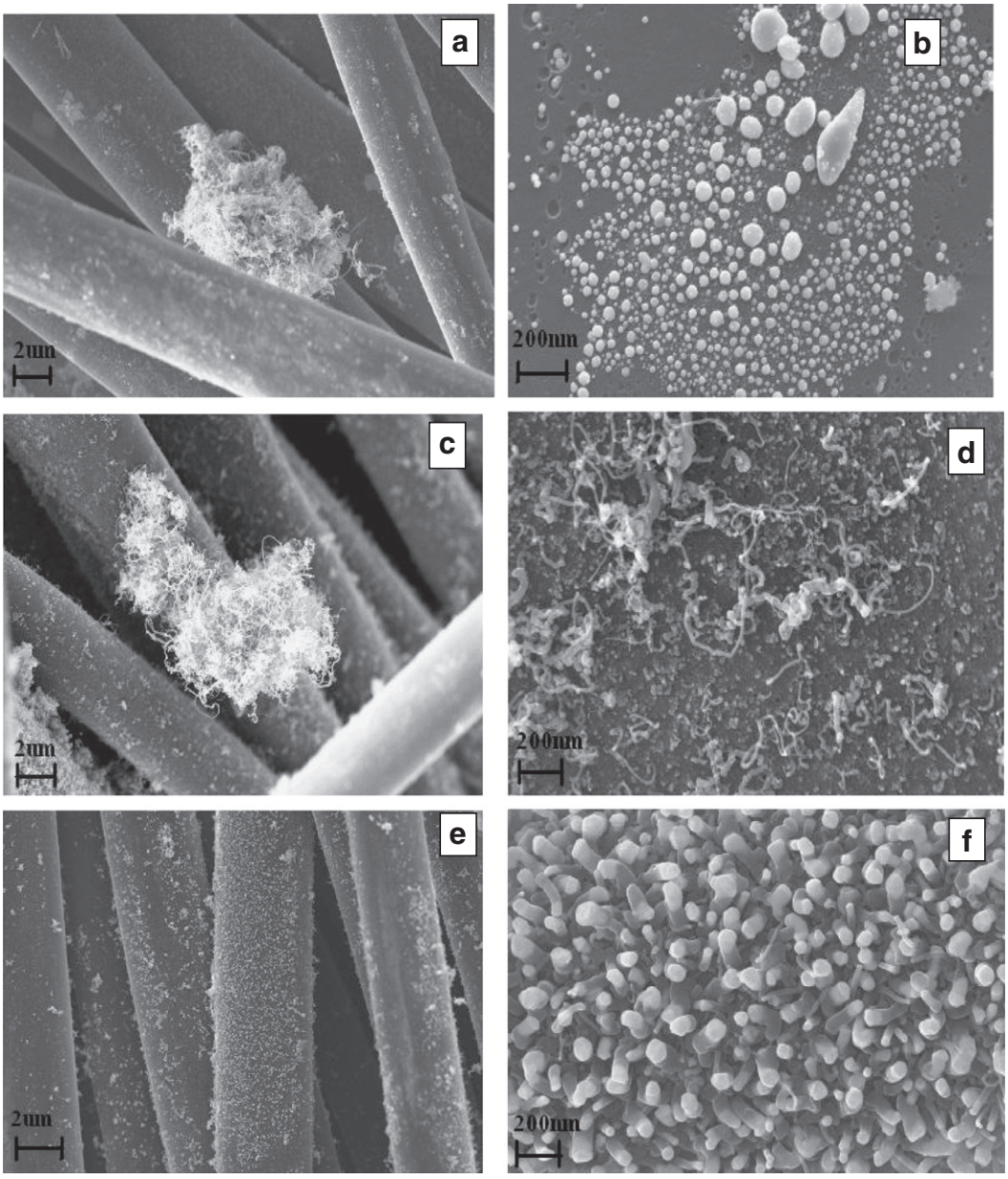

Fig. 4. SEM images of CNFs grown using different metal combinations: (a, b) Ni–Cu ACF/CNF, (c, d) Ni–Fe ACF/CNF, and (e, f) Fe–Cu ACF/CNF.

diameter of the CNF with Fe nanoparticles attached to its tip was observed to vary between 40 and 60 nm. The CNFs were also observed to have the stacked cup-structure consisting of continuous grapheme layers. Further, the fibers are in the spiral form along the fiber axis. Such morphology may be considered to be good for immobilization because enzyme may be adsorbed on the tips and on the surface of the CNFs. Fig. 4(c) and (d) show the images of CNFs after adsorption with enzyme. A discernible difference may be observed between the samples before and after adsorption. The visible black spots observed on the images in Fig. 4(d) are the enzymes immobilized on the surface and CNF tips.

4.1.4. SEM analysis

The SEM images were taken at different magnifications (5, 10, 50, 100 KX) at various locations on the samples. As mentioned earlier in this paper, different combinations (Ni and Cu, Ni and Fe, or Fe and Cu) of metals were investigated for growing dense and uniform CNFs so that one metal remained adhered on the surface and the other metal was attached on CNF tips. Fig. 4 shows the SEM images of different bimetal-grown CNFs. Insignificant growth may be observed in the web prepared using Ni and Cu, whereas the web grown using Ni and Fe is relatively less dense with fibers. Agglomeration of fibers is also observed. However, the combination of Fe and Cu metals yields a significantly larger dispersion and denser growth of CNFs than the other two combinations. Based on these results, the web of ACF/CNF was prepared using Fe and Cu.

Figs. 5(a, b) and 6(c, d) show the SEM images of the non-sonicated (Fe–Cu ACF/CNF) and sonicated (Cu-ACF/CNF) samples, respectively. The shiny Fe-metal nanoparticles may be observed on the non-sonicated sample tips, whereas the metal nanoparticles are absent on the tips of samples that were ultrasonicated. The metal nanoparticles were dislodged during sonication. The SEM images of the sonicated bimetal-grown CNFs with and without immobilization of GOx are shown in Fig. 5(e, f). The difference between the morphology

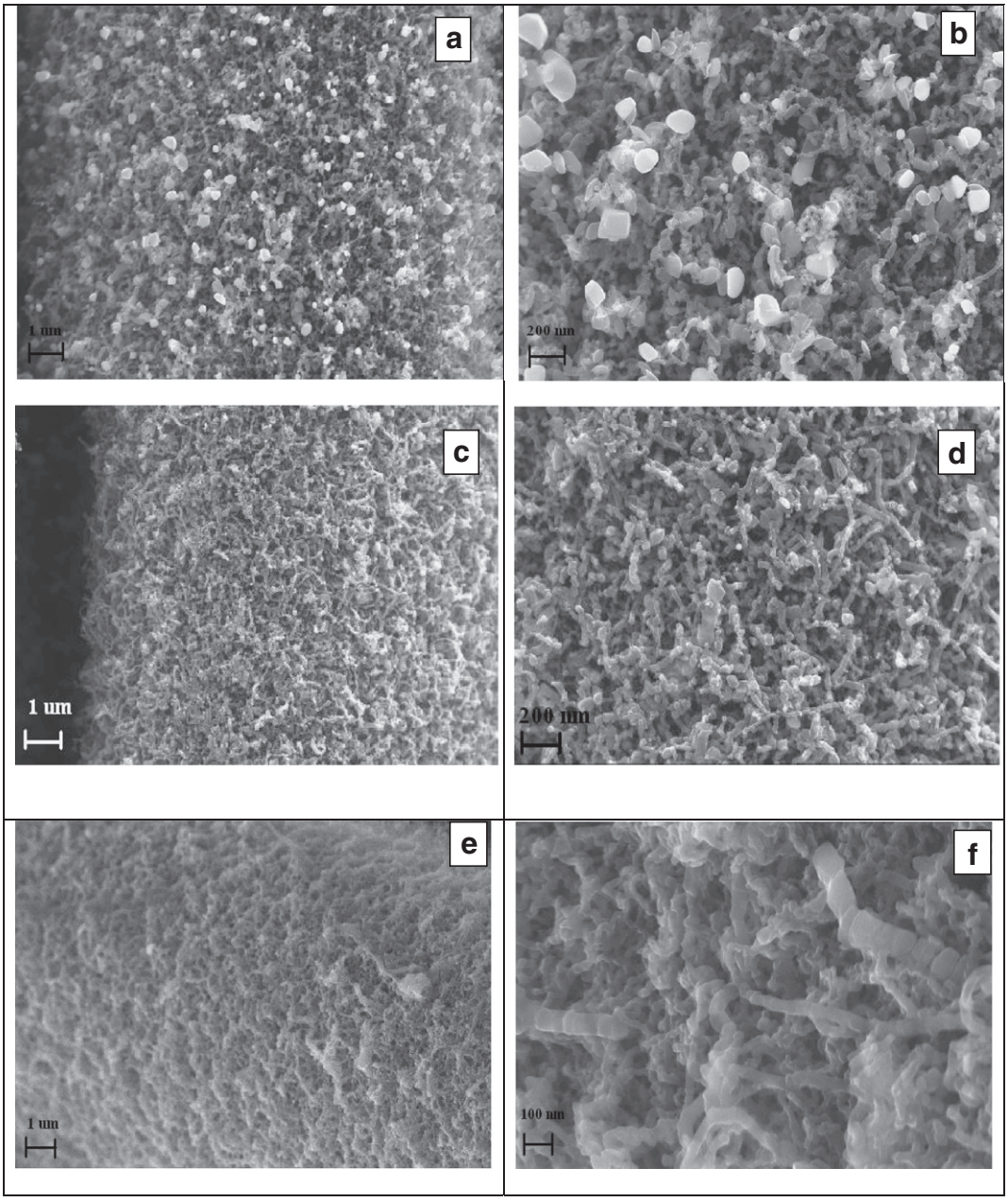

Fig. 5. SEM images of (a, b) Fe–Cu ACF/CNF, (c, d) Cu-ACF/CNF, and (e, f) enzyme adsorbed Cu-ACF/CNF samples.

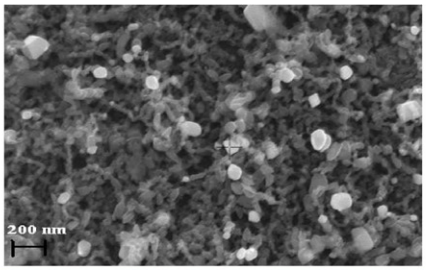

Elements	Weight %
Carbon	57.67
Oxygen	2.71
Iron	36.27
Copper	3.33

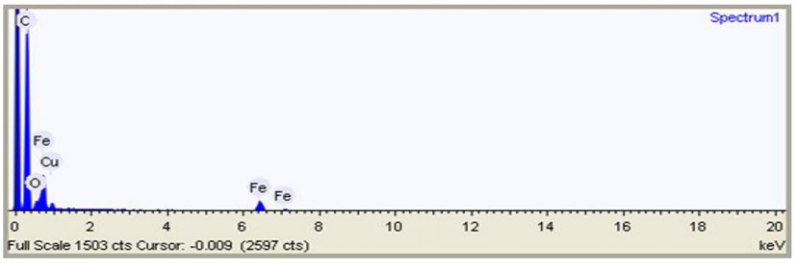

a) EDX spectrum of non-sonicated Fe-Cu ACF/CNF.

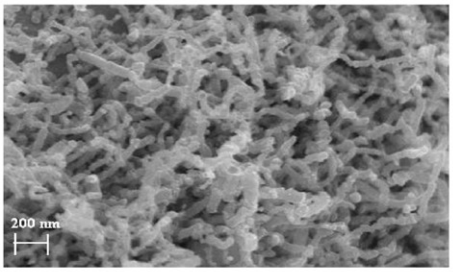

Elements	Weight %
Carbon	84.79
Oxygen	5.94
Copper	9.72

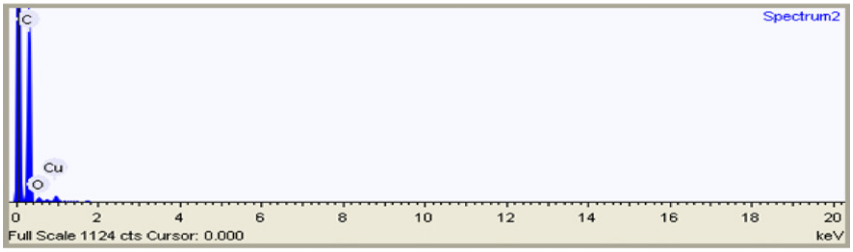

b) EDX spectrum of Cu-ACF/CNF sample after 5 min of sonication.

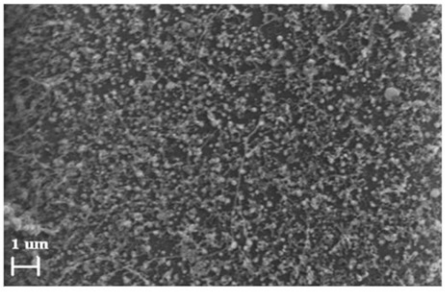

Elements	Weight %
Carbon	74.42
Oxygen	13.43
Copper	12.15

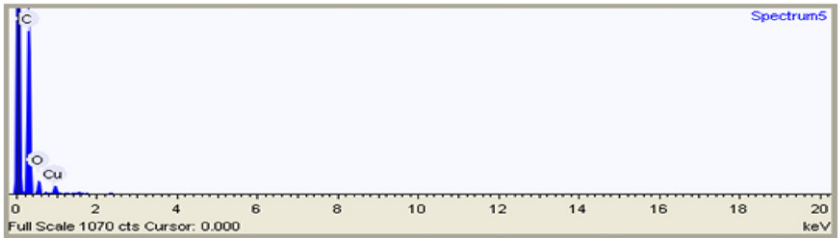

c) EDX spectrum of Fe-Cu ACF/CNF sample after 15 min of sonication.

Fig. 6. EDX spectrum of (a) non-sonicated Fe–Cu ACF/CNF, (b) Cu-ACF/CNF sample after 5 min of sonication, and (c) Fe–Cu ACF/CNF sample after 15 min of sonication.

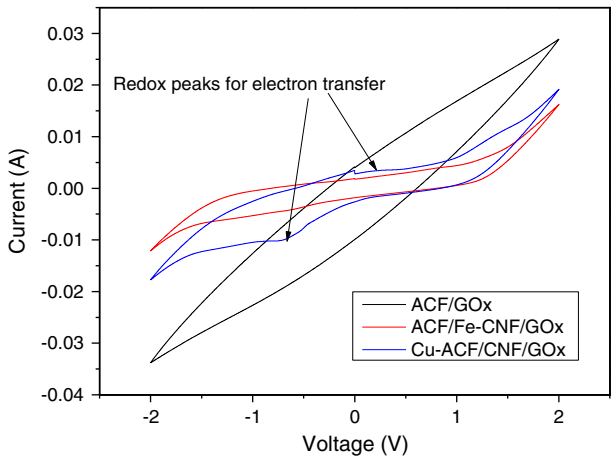

Fig. 7. CV of (a) ACF/GOx, (b) ACF/Fe-CNF/GOx, and (c) Cu-ACF/CNF/GOx (scan rate = 100 mV/s).

of CNFs before and after adsorption of enzyme may be clearly observed. The enzyme may be observed to be uniformly immobilized on both the walls and the CNF tips.

4.1.5. EDX analysis

The bimetal (Fe–Cu)-grown CNFs were analyzed by EDX, along with SEM, to confirm that CNFs were grown by the tip-growth mechanism, with Fe nanoparticles attached to the CNF tips and Cu nanoparticles adhered to the ACF substrate. The EDX spectra were taken at different locations of the prepared hierarchical structures of the non-sonicated as well as sonicated samples.

Fig. 6(a) describes the EDX spectra of the locations or spots at or near the tips of the non-sonicated CNF samples. The weight-percentages of Fe and Cu were measured to be 36.27 and 3.33, respectively, thus corroborating the fact that most of Fe-metals were attached to the CNF tips. The EDX analysis of the samples that were sonicated for different times (5 and 15 min) was also conducted to examine the type and amount of the base metal remaining in the material. It was expected that the sonication of the CNFs for longer time would result in dislodging of large amounts of metals from the tips of the fibers, along with some fibers from the ACF substrate.

Fig. 6(b) displays the SEM image and the EDX spectrum of the CNF samples after 5 min of sonication. Most of the Fe nanoparticles were removed from the tips and mostly Cu nanoparticles (9.72%) remained at the surface. Fig. 6(c) depicts the EDX spectrum of the CNF samples after 15 min of sonication. Most of the CNFs were removed from the surface of ACF, and only the base metal remained at the surface. The EDX spectra indeed confirmed that the base metal was Cu, with the overall composition of Cu nanoparticles in the samples measured to be 12.15% and no Fe-metals found on the surface of the ACF substrate.

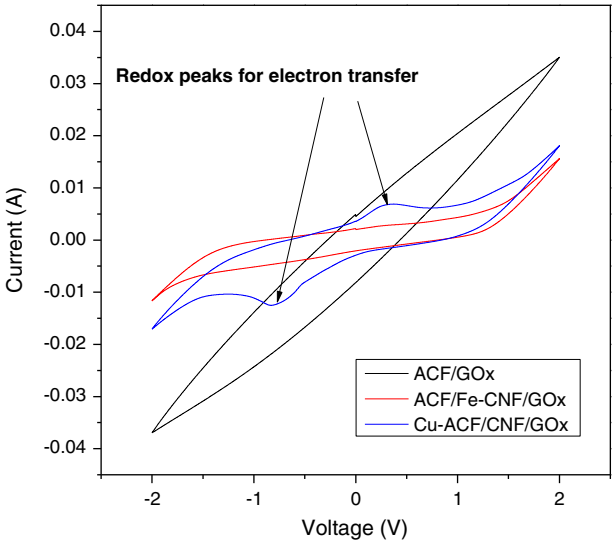

Fig. 8. CV of (a) ACF/GOx, (b) ACF/Fe-CNF/GOx, and (c) Cu-ACF/CNF/GOx in the presence of 2 mM glucose (scan rate = 100 mV/s).

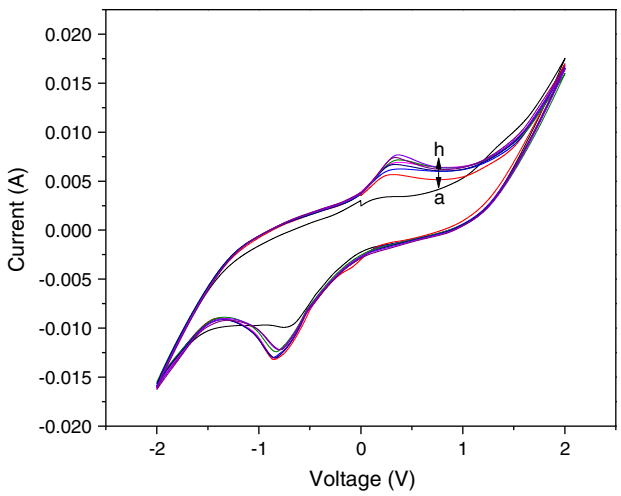

Fig. 9. CV of Cu-ACF/CNF/GOx electrode in (a) 0 mM (blank), (b) 0.5 mM, (c) 1 mM, (d) 2 mM, (e) 4 mM, (f) 6 mM, (g) 8 mM, and (h) 10 mM, in 0.05 M phosphate buffer (pH = 7) (scan rate = 100 mV/s).

4.2. Glucose biosensor

4.2.1. Comparison of CV characteristics of different materials

Fig. 7 presents the CVs of ACF, ACF/Fe-CNF and Cu-ACF/CNF composites, which were each adsorbed with GOx, in the air saturated 0.05 M PBS (pH = 7.2) electrolytes, between the voltage range of -2 V to 2 V at the scan rate of 100 mV/s. As mentioned earlier in the text, ACF/Fe-CNF/GOx represents the web of ACF/CNF prepared using single metal (Fe) catalyst nanoparticles, adsorbed with GOx after sonication.

No redox peaks were observed in the CV of ACF because ACF did not catalyze any electrochemical reaction. Therefore, it yielded only the background current. In the case of ACF/Fe-CNF/GOx, marginal

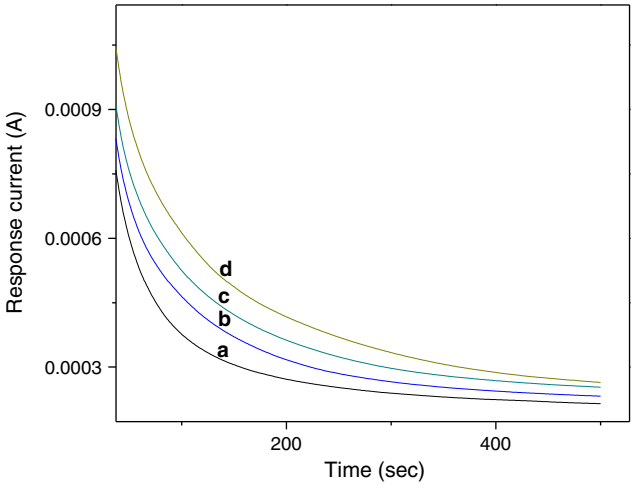

Fig. 10. Current–time curves for Cu-ACF/CNF based electrode at 0.7 V in glucose solution: (a) 0 mM (blank), (b) 1 mM, (c) 4 mM and (d) 8 mM, in 0.05 M phosphate buffer (pH = 7).

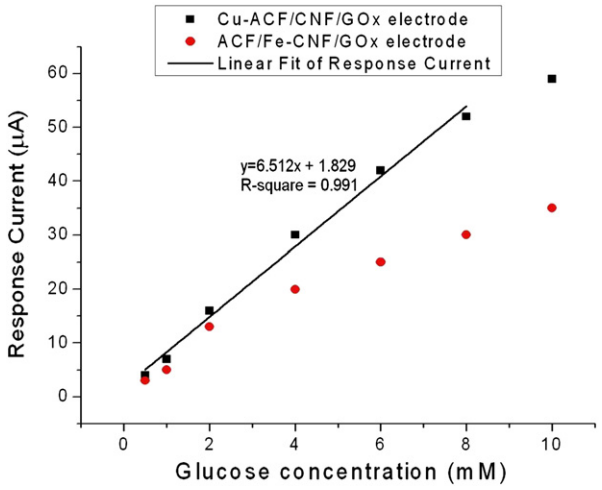

Fig. 11. Calibration curves of glucose biosensor using (a) Cu-ACF/CNF/GOx and (b) ACF/Fe-CNF/GOx electrodes.

electrochemical activity was observed. However, no clear redox peaks were observed. By contrast, the CV of bi-metal grown web of ACF/CNF having Cu nanoparticles dispersed in the ACF substrate exhibited a redox peak suggesting that the material has electro-catalyzing properties and a significant electron transfer rate.

To investigate the redox potentials of the prepared material, CVs of ACF, ACF/Fe-CNF and Cu-ACF/CNF, each adsorbed with GOx, were obtained in 2 mM glucose in 0.05 M PBS buffer (pH = 7.2) voltage ranging from −2 V to 2 Vat the scan rate of 100 mV/s. GOx catalyzes the oxidation of glucose to glucono-δ-lactone in the presence of oxygen, while the co-factor, FAD of GOx is reduced to $FADH_2$. $FADH_2$ is subsequently re-oxidized to FAD with the formation of H_2O_2 [6]. The produced H_2O_2 is detected amperometrically at 0.7 V using a platinum electrode, and the corresponding electrochemical current is related to the glucose concentration of the solution. The concerned reactions are as follows [6,25]:

$$\text{GOx (FAD)} + \text{Glucose} \rightarrow \text{GOx (FADH2)} + \text{Glucono-}\delta\text{-lactone}$$

$$\text{GOx } (FADH_2) + O_2 \rightarrow \text{GOx (FAD)} + H_2O_2$$

$$H_2O_2 \rightarrow 2H^+ + O_2 + 2e^- \text{ (at 0.7V)}.$$

The CV characteristics of different materials are shown in Fig. 8. The characteristics of ACF/GOx remained unchanged with no electrochemical or enzymatic activity. ACF/Fe-CNF/GOx had insignificant activity with negligible increase in redox peaks, whereas Cu-ACF/CNF/GOx composite demonstrated significant enzymatic activity and an electron transfer rate with a proportionate increase in the redox peaks. This behavior suggested the latter material to be a potential candidate for the electrode of a glucose biosensor.

4.2.2. Effect of glucose concentrations on oxidation peaks

Fig. 9 shows the variation in oxidation peak-current because of the oxidation of glucose at different concentrations. As observed, the current increases with increasing glucose concentrations, which is an indication of the increased oxidation rate of glucose or the enzymatic activity of the Cu-ACF/CNF/GOx electrode.

4.2.3. Amperometric detection of glucose

The noticeable performance of the ACF-supported bimetal-grown CNF-based electrode toward yielding high electron transfer rate and redox peak in the CV characterization curve makes it an attractive material for the electrode of enzymatic glucose sensors. To further examine its potential application, the amperometric response of the prepared material was examined at different glucose concentrations in the range of 0.5 mM–10 mM. The amperometric response of the glucose solution was measured at the constant potential of 0.7 V vs. Ag/AgCl reference electrode. Typical amperometric curves (current vs. time) were obtained and are displayed in Fig. 10. The response currents are observed to increase with increasing glucose concentrations.

Fig. 11 shows the calibration curves of Cu-ACF/CNF/GOx and ACF/Fe-CNF/GOx electrodes used as a working electrode in the three-electrode assembly. There are two salient results. (1) Cu-ACF/CNF/GOx having Cu nanoparticles dispersed in ACF has a greater response than that of ACF/Fe-CNF/GOx (prepared with single metal (Fe), without Cu dispersed in the substrate ACF). (2) The calibration curve is approximately linear over the large glucose concentration range used in the tests. The analysis of the data revealed that the proposed Cu-ACF/CNF/GOx-based biosensor maintains linearity (correlation coefficient = 0.991) up to 8.5 mM of glucose concentration, with a detection limit <0.5 mM and a current sensitivity of 6.512 μA/mM or 8.29 μA/mM-cm^2, based on the electrode area of 78.5 mm^2. However, the sensor using ACF/Fe-CNF/GOx-based electrode maintains linearity (correlation coefficient = 0.9775) up to 6.5 mM with a detection limit <0.5 mM and a sensitivity of 3.91 μA/mM or 4.98 μA/mM-cm^2. These data corroborate the significance of preparing a multi-scale web of carbon fibers using bimetals, with Cu nanoparticles dispersed in the ACF substrate and Fe nanoparticles attached to the tips of the grown nanofibers, the latter metal nanoparticles being subsequently replaced with enzymes during the sonication step.

The sensitivity and other characteristics of the Cu-ACF/CNF/GOx based electrode prepared in this study were also compared, wherever possible, to those discussed in the literature. Table 3 presents the comparative data, which show that the bimetal-grown ACF/CNF-based electrode developed in this study, have an enhanced sensitivity and a satisfactory linear range. As also observed from the table, its characteristics may be considered to be comparable, in most cases, to the other CNT-based glucose sensors described in the literature that were prepared using noble metals, including Au and Pt.

Here, this is important to mention that that the detection of glucose may be interfered by electroactive compounds if present in the liquids. For example, a few electroactive compounds such as urea, glycine, ascorbic acid, paracetamol and uric acid may interfere with the

Table 3
Comparison of Cu-ACF/CNF/GOx based electrode with the electrodes described in the literature.

Working electrode	Working potential (V)	Maximum concentration of linear range (mM)	Sensitivity (μA/mM[a] or μA/mM-cm^2)	Correlation Coefficient
Cu-ACF/CNF (this study)	0.70	8.5	6.51[a] or 8.29	0.991
ACF/Fe-CNF (this study)	0.70	6.5	3.91[a] or 4.98	0.978
Pt nanoparticles-supported CNTs/glassy carbon electrode [5]	0.50	4.0	0.56[a]	0.993
Pt nanoparticles supported on CNTs [6]	0.30	2.0	41.90	0.998
Pt nanoparticle–graphene nanocomposite [8]	0.40	1.5	8.20[a]	0.997
Nafion/GOx-GNP/GCE [27]	0.27	6.0	6.50	0.99
Chitosan modified CNTs [28]	0.40	7.8	0.52	–

[a] The sensitivity not reported on the electrode-area basis.

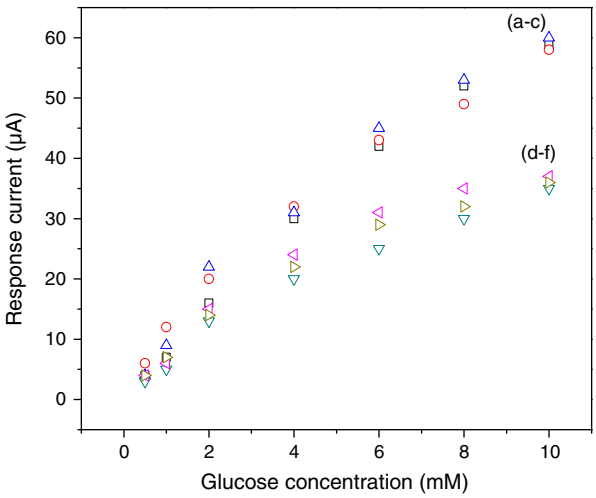

Fig. 12. Reproducibility results of glucose sensor using (a–c) ACF/bi-metal CNF/GOx and (d–f) ACF/Fe-CNF/GOx electrodes.

detection of glucose, if present in blood serum [26]. The interference tests are very extensive [29,30] and will be conducted in a separate study.

4.2.4. Reproducibility

Reproducibility is an essential aspect of a sensor in that it determines its application in detecting the species multiple times with maximum accuracy. To study the reproducibility of the prepared electrodes, Cu-ACF/CNF and ACF/Fe-CNF samples adsorbed with GOx were tested three times under identical operating conditions. The amperometric response of each electrode was measured separately. Fig. 12 shows the calibration/response curves of two electrodes after enzyme adsorption. The data show reproducibility within the maximum 12% variation for each case.

5. Conclusions

A novel multi-scale web of carbon micro-nanofibers was prepared by catalytic CVD using Fe and Cu metal nanoparticles. In such a web, Cu was adhered to the ACF substrate and Fe was attached to the tip of CNFs. The combination of Fe and Cu in the molar ratio of 3:1 was found to yield dense and uniform CNFs at the CVD temperature of 800 °C. The prepared web was used as an effective immobilizing matrix for the GOx after ultrasonication. The prepared Cu-ACF/CNF/GOx composite was effectively applied as the working electrode of a biosensor for detecting glucose, with a sensitivity of 8.29 μA/mM-cm^2 and a linearity up to 8.5 mM ($R^2 = 0.991$). In most cases, these results are comparable to the CNT/CNF-based glucose biosensors discussed in the literature. The method of developing the ACF/CNF web as the electrode for the glucose biosensors using transition metals (Fe and Cu) is novel, simple, and cost-effective.

Acknowledgments

The authors acknowledge the support from DBT (New Delhi, India) in the form of a research grant and DST (New Delhi, India) through its Unit of Excellence on Soft Nanofabrication.

References

[1] S.B. Bankar, M.V. Bule, R.S. Singhal, L. Ananthanarayan, Biotechnol. Adv. 27 (4) (2009) 489.
[2] S. Borgmann, A. Schulte, S. Neugebauer, W. Schuhmann, Amperometric Biosensors, in: R.C. Alkire, D.M. Kolb (Eds.), Advances in Electrochemical Science and Engineering, Wiley-VCH, 2011, p. 1.
[3] J. Wang, Electroanalysis 17 (1) (2005) 7.
[4] B.P. López, M. Guix, S. Alegret, A. Merkoçi, IBER SENSOR 2008 Conference, 24–26 November, São Paulo, Brasil, 2008.
[5] H.J. Wang, C.M. Zhao, F. Peng, H. Yu, Int. J. Electrochem. Sci. 2 (2007) 508.
[6] W. Li, R. Yuan, Y. Chai, H. Zhong, Y. Wang, Electrochim. Acta 56 (2011) 4203.
[7] M.E.G. Lyons, G.P. Keeley, Int. J. Electrochem. Sci. 3 (2008) 819.
[8] H. Wu, J. Wang, X. Kang, C. Wang, D. Wang, J. Liu, I.A. Aksay, Y. Lina, Talanta 80 (1) (2009) 403.
[9] D. Shan, S. Wang, Y. He, H. Xue, Mater. Sci. Eng. C 28 (2008) 213.
[10] X. Ren, X. Meng, F. Tang, L. Zhang, Mater. Sci. Eng. C 29 (2009) 2234.
[11] W. Nouira, A. Maaref, H. Elaissari, F. Vocanson, M. Siadat, N. Jaffrezic-Renault, Mater. Sci. Eng. C 33 (2013) 298.
[12] S. Adapa, V. Gaur, N. Verma, Chem. Eng. J. 116 (1) (2006) 25.
[13] V. Gaur, R. Asthana, N. Verma, Carbon 44 (2006) 46.
[14] V. Gaur, A. Sharma, N. Verma, Carbon 15 (15) (2005) 3041.
[15] L. Xu, J. Guo, F. Jin, H. Zeng, Chemosphere 62 (2006) 823.
[16] A. Hui, B. Feng, S. Shi, Int. J. Greenhouse Gas Control 5 (1) (2011) 16.
[17] C. Yang, K. Kaneko, J. Colloid Interface Sci. 255 (2002) 236.
[18] R. Singhal, A. Sharma, N. Verma, Ind. Eng. Chem. Res. 47 (10) (2008) 3700.
[19] A. Gupta, D. Deva, A. Sharma, N. Verma, Ind. Eng. Chem. Res. 49 (15) (2010) 7074.
[20] A. Chakraborty, D. Deva, A. Sharma, N. Verma, J. Colloid Interface Sci. 359 (1) (2011) 228.
[21] H. Katepalli, B. Mekala, C.S. Sharma, N. Verma, Chem. Eng. J. 171 (3) (2011) 1194.
[22] D. Lozano-Castello, D. Cazorla-Amoros, A. Linares-Solano, Carbon 42 (2004) 1231.
[23] S. Libertino, V. Aiello, A. Scandurra, M. Renis, F. Sinatra, Sensors 8 (9) (2008) 5637.
[24] D. Li, Q. He, Y. Cui, L. Duan, J. Li, Biochem. Biophys. Res. Commun. 355 (2) (2007) 488.
[25] A. Keyhanpour, S.M.S. Mohaghegh, A. Jamshidi, Biosens. Bioelectron. 3 (1) (2012) 1.
[26] D.R.S. Jeykumari, S.S. Narayanan, Biosens. Bioelectron. 23 (2008) 1404.
[27] S. Zhao, K. Zhang, Y. Bai, W.W. Yang, C. Sun, Bioelectrochemistry 69 (2) (2006) 158.
[28] Y. Liu, M.K. Wang, F. Zhao, Z.A. Xu, S.J. Dong, Biosens. Bioelectron. 21 (2005) 984.
[29] R.H. White-Stevens, Clin. Chem. 28 (4) (1982) 587.
[30] D. Moatti-Sirat, G. Velho, Biosens. Bioelectron. 7 (5) (1992) 345.